Comparing Various Concentrations of 1,3,4-*O*-Bu_3ManNAz on Incorporation into the Sialic Acid Pathway in CHO-K1 Cells

Zan Chaudhry Partner: Eric Simon

Cell and Tissue Engineering Lab, Spring 2023 10:30 AM

Introduction

Metabolic glycoengineering (MGE) is a developing method for modifying glycosylation pathways.[1] Glycosylation refers to the attachment of carbohydrates to other macromolecules to modulate their functions and demonstrates the diverse role of sugars outside of metabolism.[2] In particular, glycosylation of cell-surface proteins has been implicated in a wide variety of cellular activities, from cell-to-cell communication to infection. In MGE, sugar inputs to the cell are altered to produce altered glycans on the cell surface, which can introduce novel cell functionalities. For example, the hemagglutinin protein expressed by influenza complexes with sialic acid, a ubiquitous sugar found at the ends of glycan chains on cell-surface glycoproteins, allowing the virus to attach to and infect cells.[1] Modification of these sialic acids by replacing the input sugar in this pathway (ManNAc) with analogous, modified sugars can produce structurally distinct surface sugars, preventing influenza infection. Thus, MGE presents a method for utilizing relatively simple molecules (carbohydrates) as therapeutics and presents a pathway for understanding the less-explored "glyco-sphere" of functional carbohydrates in the cell.[3]

Investigation of the sialic acid pathway remains a topic of exploration in MGE, and a variety of modified ManNAc analogs have been studied. 1,3,4-*O*-Bu_3ManNAz is an analog of particular interest for its high incorporation efficiency and potential for cell labeling through "click chemistry" reactions involving the azide group.[1] Characterizing the properties of analogs such as 1,3,4-*O*-Bu_3ManNAz is an important step in the development of MGE techniques. The following report presents such a characterization, varying concentrations of 1,3,4-*O*-Bu_3ManNAz in cultured CHO-K1 cells to investigate incorporation efficiency and cytotoxicity. Six analog concentrations are investigated: 50, 90, 130, 170, 210, and 250 μM. The researchers hypothesize that the 250 μM cells will display the greatest incorporation efficiency and cytotoxicity and that, in general, incorporation efficiency will increase with increasing concentration due to greater availability of sugar analog and that cytotoxicity will increase with increasing concentration due to greater volumes of ethanol (the solvent in which the analog is stored), which is potentially harmful to cells.

Methods

Cell Line Details

Cells used in the following experiments were the seventh passage (passaged every 2-3 days) of a CHO-K1 (ATCC; Manassas, VA) cell culture acquired and maintained prior to the start of the experiments. These cells were originally grown in DMEM/F-12K, HEPES growth media containing 10%

fetal bovine serum (heat-inactivated) and both penicillin and streptomycin (to prevent bacterial contamination) in an incubator set to 37 °C / 5% CO_2. However, FBS interferes with MGE, and thus serum-free media (same composition otherwise) was used for the following experiments.

Cell Seeding

Six different cell counts (19, 38, 76, 115, 153, and 192 thousand cells per well) were plated with serum-free media and incubated for 48 hours to determine the optimal (achieving ~90% confluency after 48 hours) cell count to plate for the MGE experiments. Confluency and cell health were examined at the end of incubation by microscopy, and the optimal cell count was found to be 38,000 cells per well.

Metabolic Analog Incorporation

Concentrations of 50, 90, 130, 170, 210, and 250 μM 1,3,4-*O*-Bu_3ManNAz were tested. These solutions were made from a 100 mM azide analog in ethanol stock solution (Yarema Lab; Baltimore, MD). A 24-well plate (Table 1) was seeded with 38,000 cells per well. Three control groups were prepared: untreated cells, untreated cells with fluorescent tag (the fluorescent tag was added during analysis, so this group is the same as untreated cells during plating), and cells treated with the maximum ethanol volume from the experimental groups (2.5 μL per well).

	1	2	3	4	5	6
A	0.5 μL analog	0.5 μL analog	0.5 μL analog	0.9 μL analog	0.9 μL analog	0.9 μL analog
B	1.3 μL analog	1.3 μL analog	1.3 μL analog	1.7 μL analog	1.7 μL analog	1.7 μL analog
C	2.1 μL analog	2.1 μL analog	2.1 μL analog	2.5 μL analog	2.5 μL analog	2.5 μL analog
D	CHO-K1	CHO-K1	CHO-K1*	CHO-K1*	2.5 μL EtOH	2.5 μL EtOH

Table 1: Plating strategy for MGE experiments. Each experimental condition was plated in triplicate (the volume of 100 mM azide analog added to each well is shown). Row D contains the control groups plated in duplicates, with CHO-K1 referring to untreated cells. A * indicates the control wells that received incubation with the fluorophore during analysis. A stock solution of four wells-worth of cells, media, and analog was prepared for each condition to minimize errors due to pipetting inaccuracies.

Analysis

Media was removed, and cells were fixed with 4% paraformaldehyde in PBS. Nuclei were stained with Hoechst 33342 dye (Bio-Rad; Hercules, CA) at a concentration of 40 μg/mL, diluted with PBS from a stock solution at 10 mg/mL. The stain was aspirated, wells were rinsed with 2% bovine serum albumin (BSA) in PBS solution, and a Click-iT buffer with alkyne-bound AlexaFluor488 was added for fluorescent labeling of azide analogs. This solution was aspirated and rinsed with BSA in PBS, and fresh PBS was added to wells for analysis. A representative slice of each condition was captured with DAPI filter to provide cell viability. These images were processed by subtracting background, converting to binary, and median filtering. Viability was calculated by dividing the number of nuclei (software counted) present in each slice by the number of nuclei present in the control. The same slices were imaged with GFP filter to qualitatively assess analog spatial localization. Additionally, overall AlexaFluor488 fluorescence data was collected with a microplate reader (excitation/emission: 485/528 nm).

Reagents and Equipment

Except where otherwise stated, reagents/materials were purchased from Thermo Fisher Scientific (Waltham, MA). A Countess II (Thermo Fisher; Waltham, MA) was used for cell counting. An EVOS M5000 (Life Technologies; Waltham, MA) was used for microscopy. Fiji (ImageJ ver. 1.54b) was used for image analysis.[4] A Synergy 2 (Agilent; Santa Clara, CA) was used for fluorescence reading.

Results

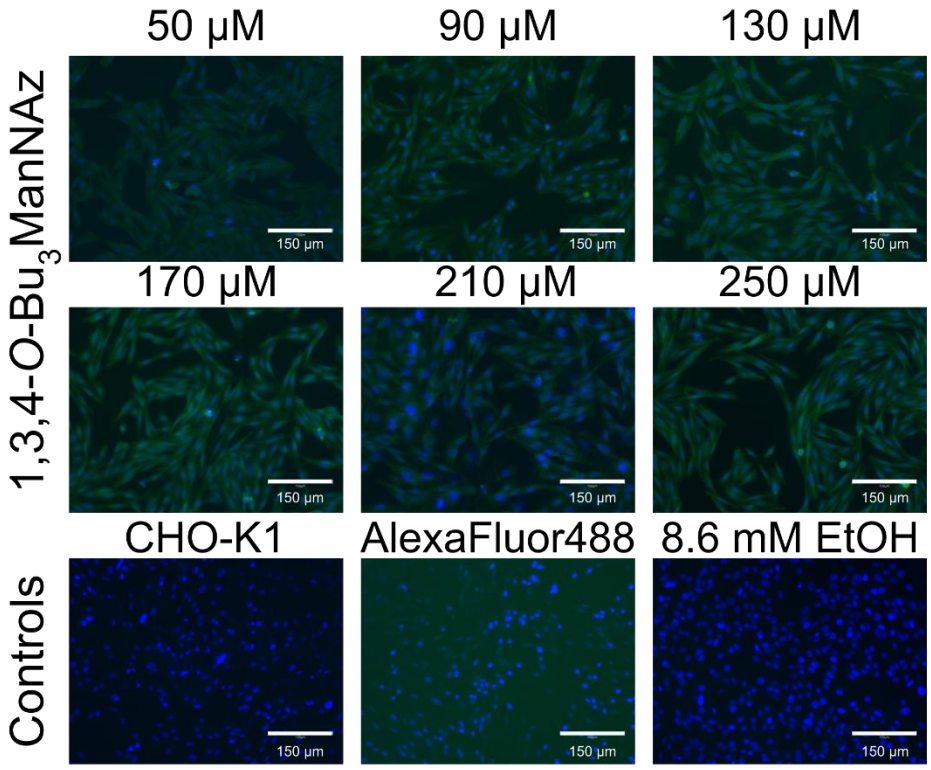

Figure 1: Composite microscope images for each condition. Green channel corresponds to GFP filter (highlighting regions of analog incorporation illuminated by bound AlexaFluor488) and blue channel corresponds to DAPI filter (highlighting Hoechst-stained nuclei). Scale bar is 150 µM in all images.

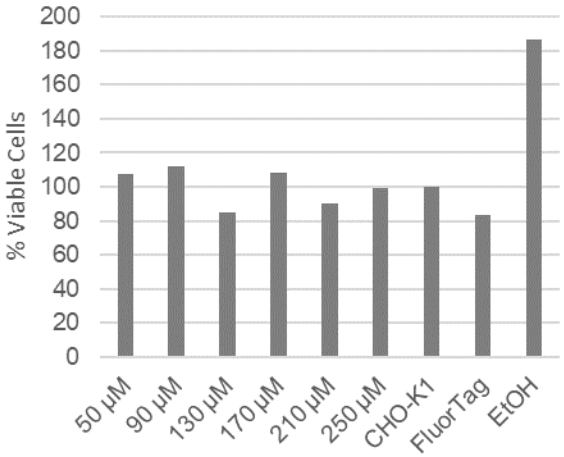

Figure 2: Cell viability by condition. FluorTag refers to control cells exposed to AlexaFluor488/Click-iT buffer.

Composite microscopy images (Fig. 1) illustrate successful analog incorporation in all experimental groups, no analog incorporation in untreated cells and ethanol control groups, and some fluorophore activity in the control group treated with AlexaFluor488. Experimental groups display spatial localization of fluorescence activity along cell surfaces. The fluorophore-treated control group, however, displays a homogeneous layer of fluorescence without any spatial distinctions. From the images, the intensity of the green channel is similar in the 90, 130, 170, and 250 µM conditions, but markedly lower in the 50 and

210 μM conditions. Cells display a healthy, elongated morphology without signs of overcrowding in the experimental groups (as illuminated by fluorophore bound to cell surfaces). The control groups displayed similar cell morphology/health under transmitted light (not shown).

Cell viability calculations (Fig. 2) displayed two key findings. There was no visible trend relating analog concentration with cytotoxicity, with three groups displaying viabilities above the control (50, 90, and 170 μM), and three below (130, 210, and 250 μM), with no pattern to the groups above and below. Additionally, the ethanol-treated control group displayed a substantially higher viability than all other groups (187%). Since these were single-trial measurements, significance cannot be assessed, however Z-scoring can be performed by taking the mean and standard deviation of all of the cell viabilities. The ethanol-treated group's 186% produces a Z-score of 2.51, indicating that 99.4% of samples pulled from a normal distribution constructed from the cell viability data would be less than 186%.

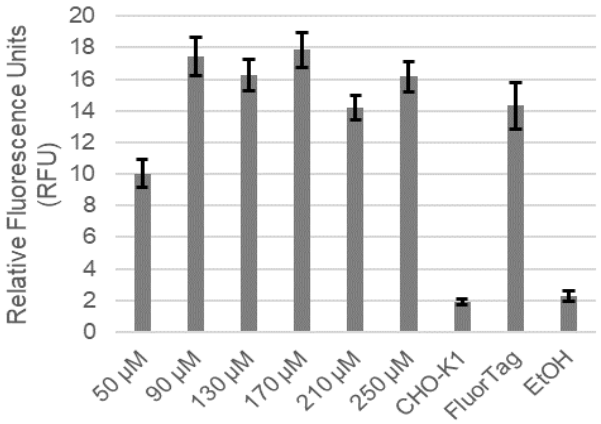

Figure 3: Relative AlexaFluor488 fluorescence readings by condition. FluorTag refers to control cells exposed to fluorophore / Click-iT buffer. Bars indicate 95% confidence interval calculated by Student's t-distribution.

Finally, the microplate reader data (Fig. 3) displayed trends consistent with the microscopy. All experimental groups displayed statistically significant increases in fluorescence relative to the untreated and ethanol controls by t-test ($p < 0.05$). Differences in fluorescence readings for the 90, 130, 170, and 250 μM are statistically insignificant ($p > 0.05$, as evidenced by overlapping 95% t-distribution confidence intervals on Fig. 3), suggesting that these four concentrations produced roughly the same level of analog incorporation (like what was seen in microscopy). Additionally, the difference in fluorescence readings between both the 50 μM and 210 μM groups and all other experimental conditions was statistically significant by t-test ($p < 0.05$), mirroring the markedly lower fluorescence relative to the other groups seen in the microscopy for these two groups. The difference in fluorescence between the ethanol and untreated cells control groups was statistically insignificant by t-test ($p < 0.05$), again agreeing with microscopy. Finally, several experimental groups (130, 210, and 250 μM) displayed insignificant differences in fluorescence (by t-test) with the fluorophore-incubated control, also as seen in Fig. 1.

Discussion

Prior to the experiments, it was hypothesized that increasing 1,3,4-*O*-Bu_3ManNAz concentration would increase the level of sugar analog incorporation into the sialic acid pathway. The data partially supports this hypothesis. Analog incorporation (as measured by fluorescence) increased from the control to the 50 μM group and from the 50 μM to the 90 μM group (both differences significant by t-test);

however, beyond this point, increasing concentration did not produce significant increases in analog incorporation. This may suggest saturation of the sialic acid pathway at the 90 μM concentration of analog, after which additional sugar analog fails to produce additional glycosylation. This result disagrees with the literature, which supports the hypothesis that increasing analog increases incorporation.[5] The second portion of the hypothesis predicted increasing cytotoxicity with increasing analog concentration (due to increasing ethanol concentration). The data supports rejection of this hypothesis, as no trend was visible relating analog concentration with cytotoxicity, and in fact the ethanol-treated control group experienced the highest cell viability, contrary to the proposed ethanol-induced cytotoxicity.

The ethanol-treated control group's exceptionally high viability (186%) likely indicates a poor choice of imaging slice. The 250 μM condition contained approximately the same amount of ethanol as the ethanol control, but displayed a much more consistent viability (99%). Z-scoring ($Z = 2.51$ for the ethanol control's viability) suggests that the observed slice is an outlier, taken from too dense a region of the well; however, since only one viability measure was taken, it is difficult to draw conclusions.

Interestingly, the fluorophore-incubated control group displayed a strong fluorescence signal (a statistically significant increase over the other two controls and the 50 μM condition), though microscopy data suggests that this was likely due to experimenter error. Comparing images between the fluorophore-incubated control and the experimental groups clearly shows differences in spatial localization. In the control, the fluorescence is equally spread throughout the slice, while it is concentrated on cell surfaces in the experimental groups. This difference suggests a failure to completely wash the fluorophore solution out of the control wells, since, if it was the case that the fluorophore was binding something in the control well, we would see the same background fluorescence in the experimental groups, which is not observed.

A final anomalous point was the decrease in fluorescence observed for the 210 μM condition. Considering the plateau effect seen in fluorescence after 90 μM, from which the 210 μM value deviates, most likely the decrease resulted from experimenter error in production of the 210 μM stock solution.

Overall, the microscopy and fluorescence data presented complementary results, with the same trends (or lack thereof) visible in both modalities (see **Results**). The microscopy data demonstrates the cell-surface localization that is indicative of incorporation of the sugar analog into cell-surface glyans in the sialic acid pathway, which is quantified by the fluorescence readings.

The presented experiments measured the effect of varying 1,3,4-*O*-Bu_3ManNAz concentration on incorporation into the sialic acid pathway of CHO-K1 cells. The results suggest an initial increase in incorporation with increasing azide analog concentration, followed by a plateau above 90 μM. Overall, this report presents a framework for the testing of analog incorporation in metabolic glycoengineering experiments using click-chemistry, which paves the way for exploration of the "glyco-sphere" of functional carbohydrates in mammalian cells.

References

[1] C. Agatemor, M. Buettner, R. Ariss, K. Muthiah, C. T. Saeui and K. J. Yarema, "Exploiting metabolic glycoengineering to advance healthcare," *Nature Reviews Chemistry,* vol. 3, pp. 605-620, 2019.

[2] C. Reily, T. J. Stewart, M. B. Renfrow and J. Novak, "Glycosylation in health and disease," *Nature Reviews Nephrology,* vol. 15, pp. 346-366, 2019.

[3] K. Dammen-Brower, P. Epler, S. Zhu, Z. J. Bernstein, P. R. Stabach, D. T. Braddock, J. B. Spangler and K. J. Yarema, "Strategies for Glycoengineering Therapeutic Proteins," *Frontiers in Chemistry,* vol. 10, p. 863118, 2022.

[4] J. Schindelin, I. Arganda-Carreras, E. Frise, V. Kaynig, M. Longair, T. Pietzsch, S. Preibisch, C. Rueden, S. Saalfeld and B. Schmid, "Fiji: An open-source platform for biological-image analysis," *Nature Methods,* vol. 9, pp. 676-682, 2012.

[5] R. T. Almaraz, U. Aich, H. S. Khanna, E. Tan, R. Bhattacharya, S. Shah and K. J. Yarema, "Metabolic Oligosaccharide Engineering with N-Acyl Functionalized ManNAc Analogues: Cytotoxicity, Metabolic Flux, and Glycan-display Considerations," *Biotechnology and Bioengineering*, vol. 109, no. 4, pp. 992-1006, 2011.